

ARGONNE NATIONAL LABORATORY  
9700 South Cass Avenue, Argonne, Illinois 60439

---

**Calculation of the evolution of the fuel microstructure in UMo alloys and  
implications for fuel swelling\***

---

**J. Rest and G. L. Hofman**  
**Argonne National Laboratory**  
**U.S.A**

**and**

**I. Konovalov and A. Maslov**  
**Bochvar Institute**  
**Russia**

September 1999

To be presented at the 22nd International Meeting on Reduced Enrichment for Research and Test Reactors  
(RERTR) October 3 - October 8, 1999, Budapest, Hungary

The submitted manuscript  
has been authored by a  
contractor of the U. S.  
Government under contract  
NO. W-31-109-ENG-38.  
Accordingly, the U. S.  
government retains a  
nonexclusive royalty-free  
license to publish or  
reproduce the published form  
of this contribution, or allow  
others to do so, for  
U. S. Government purposes.

# Calculation of the evolution of the fuel microstructure in UMo alloys and implications for fuel swelling

J. Rest, G. L. Hofman, I. Konovalov, and. A. Maslov

## ABSTRACT

The evolution of a cellular dislocation structure and subsequent recrystallization have been identified as important aspects of the irradiated UMo alloy microstructure that can have a strong impact on dispersion fuel swelling. Dislocation kinetics depends on the preferential bias of dislocations for interstitials compared to vacancies. This paper presents theoretical calculations for the evolution of a cellular dislocation structure, and recrystallization in U-10Mo. Implications for fuel swelling are discussed.

### 1. Introduction

One of consequences of irradiation damage of uranium-alloy dispersion fuels for the RERTR is the formation of interstitial loops, which with increasing damage pass from a chaotic to an ordered arrangement forming a linear, or cellular (“brick”) structure. At larger doses the structure evolves to one characteristic of deformed metals: the body of a cell practically free of dislocations with the cell walls consisting of an extremely high dislocation density. Recrystallization, or grain subdivision, may occur as final result of dislocation accumulation.

A surprising feature of recrystallized fuels, such as  $\text{UO}_2$ ,  $\text{U}_3\text{O}_8$ , UC, and uranium alloys irradiated at different temperatures and damage rates is that the size of the recrystallized grains is approximately of the same order of several tenths of a micron.

Recrystallization results in the formation of a very ramified border structure that leads to acceleration of point defect transport that is equivalent to an increase of irradiation temperature and may result in enhanced gas-bubble swelling.

In the absence of recrystallization, very high dislocation densities can lead to a vacancy supersaturation and bias-driven swelling. Bias-driven swelling, or void swelling, can lead to highly unstable fuel swelling.

The theoretical analyses considers two types of dislocations – mobile (mainly loops) and immobile (forest, tangled, locked) dislocations. It is reasonable to connect the formation of cellular structure with mobile dislocations and recrystallization with the accumulation of immobile dislocations.

## 2. Model for dislocation cell formation.

Two modeling approaches, one based on dislocation mechanics, and one on energy minimization were used in order to estimate the parameters of the cellular dislocation structure.

The mechanical approach considers the formation of a cellular dislocation structure as a process of loop glide in a stress field caused by dislocation congestion on planes surrounding a cell. The gliding can be "instant" if the force of interaction is more than the force of friction in the lattice, i.e. athermal. Data for uranium show a small change of cell size ( $\sim$  a factor of 2) for an increase of irradiation temperature from  $-195$  to  $+350^{\circ}\text{C}$  (increase of relative temperature from 0.05 up to 0.45) [Hudson, 1962, 1964; Buckley, 1966]. This data supports the dominance of an athermal gliding mechanism in this temperature range.

The mechanical analysis leads to an estimate of the cell size,  $L$ , that is proportional to the ratio of the energy of an atom near a dislocation line to the total energy required to overcome Peierl's barrier and the bond energy of a dislocation with an impurity. As interatomic forces determine these energies, the above ratio will be similar for different materials, and to a first approximation independent of materials properties and temperature. The estimated value of  $L$  without pinning of dislocations by impurities is on the order of  $400a$ , where  $a$  is interatomic distance, or about 0.1-0.2 microns. If we introduce the interaction energy with impurities, the calculated cell size decreases at low temperatures. A calculation of the cell size (with impurity pinning included) as a function of temperature (interaction energy between dislocation and impurities is 0.2 eV) is shown in Fig.1. The results of the calculation shown in Fig. 1 are in qualitative agreement with the data.

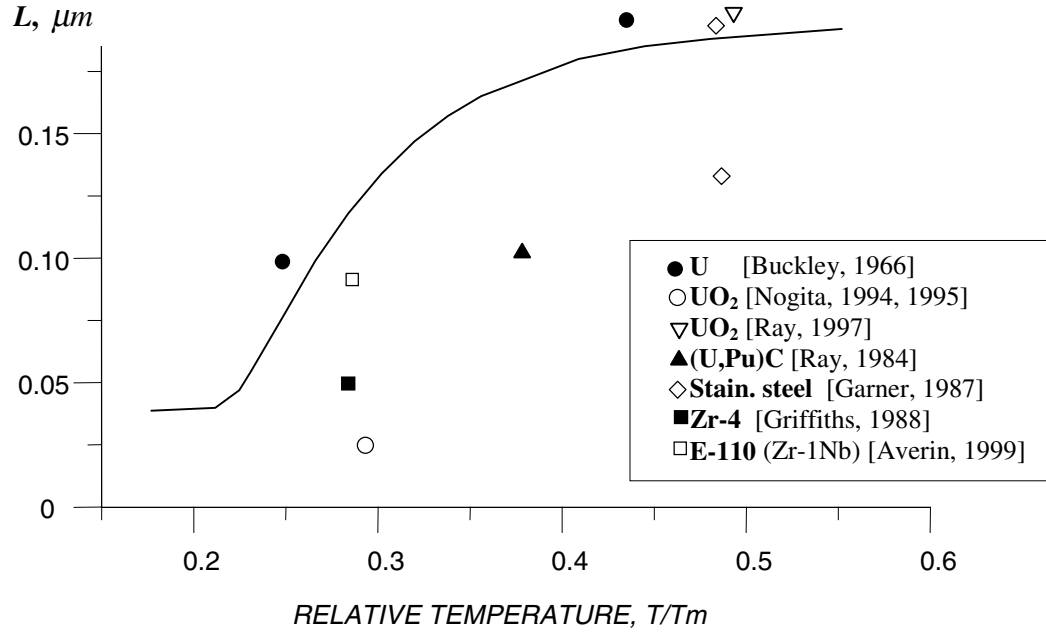


Fig.1. Comparison of calculated temperature dependence of the cell size using the mechanical approach with experimental data for fissile and structural materials.

The calculation of loop behavior within a cellular dislocation substructure that accounts for the elastic interaction of loops with tangled dislocations located on the cell walls and the rapid glide of loops to the walls results in the following main results:

- A steady-state density of mobile dislocations occurs at a fission density of about of  $10^{19} \text{ cm}^{-3}$ ;
- The steady-state density of mobile dislocations does not depend on the initial dislocation density and exhibits a weak dependence on irradiation temperature and fission rate that corresponds to the basic rules formulated for structural materials [Garner, 1982].

Analytical simplifications result in a rather simple expression for the steady-state density of mobile dislocations:

$$\rho_d = \left( \frac{6}{La} \right)^{2/3} \left( \frac{\alpha_i}{D_i} \right)^{1/3} \left( \frac{KD_v}{\alpha_r} \right)^{1/6}, \quad (1)$$

where  $K$  is the damage rate,  $\alpha_i$  and  $\alpha_r$  are the coefficients for loop nucleation (i.e., a loop nucleus is formed by a di-interstitial) and recombination coefficient, respectively, and  $D_v$  and  $D_i$  are the diffusion coefficients for vacancies and interstitials.

Using  $a=3 \cdot 10^{-8} \text{ cm}$ ,  $L=2 \cdot 10^{-5} \text{ cm}$ ,  $\alpha_i$  and  $\alpha_r$  of the order of  $10^{16} \text{ cm}^{-2}$ , we obtain the expression [ $\text{cm}^{-2}$ ]

$$\rho_d = 10^{12} K^{1/6} \frac{D_v^{1/6}}{D_i^{1/3}}. \quad (2)$$

A comparison between the calculated results using Eq. (2) (the migration energy in eV for vacancies and interstitials  $\varepsilon_{mv} = 7.8kT_M$  and  $\varepsilon_{mi} = 1.2kT_M$ ) and data for stainless steel is given in Table 1. As is demonstrated in Table 1, the calculated mobile dislocation

**Table 1. Comparison of experimental and calculated (Eq. (2)) mobile dislocation densities in stainless steel.**

The characteristics of irradiation	Average irradiation temperature, °C	Experimental meanings of dislocation density, $\times 10^{10} \text{cm}^{-2}$	Calculated meanings of dislocation density, $\times 10^{10} \text{cm}^{-2}$
BOR-60 $K \sim 10^{-6}$ dpa/s [Agapova, 1982]	400	1.6-2.1	1.8
	500	1.9-3.2	2.5
	600	1.2-3.2	3.2
Dounray Fast Reactor $K \sim 10^{-6}$ dpa/s [Brown, 1974]	500	2-5	2.5
	600	2-3	3.2
Ion irradiation $K \sim 10^{-3}$ dpa/s [Hudson, 1976]	525	8-13	8.3
	600	6-20	10
Ion irradiation $K \sim 10^{-5}$ dpa/s [Azam, 1974]	600	3-4.3	4.7

density is in reasonable agreement with the data over a relatively wide range of damage rates and temperatures.

A relationship between the cell size and the dislocation density can also be derived based on an energy minimization approach [Hanson, 1986]. According to this approach, the dislocation loops accumulate and ultimately evolve into a low-energy cellular dislocation structure. The dislocation line energy in the dislocation cell walls is given by

$$U_D = \frac{G_s b^2 f(v)}{4\pi} \ln \left( \frac{C_p C_A}{L \rho b} \right), \quad (3)$$

where  $G_s$  is the shear modulus,  $b$  is the burgers vector,  $L$  is the cell size, and it is assumed that forest dislocations primarily inhabit the cell walls. In addition, longer-range stresses of isolated terminating dislocation lines do not act with full force near the cell wall, and in a cell structure they are largely screened by the surrounding cell walls at a distance  $L$ . A reasonable estimate for the energy per unit volume stored in them is

$$U_w = \frac{G_s}{2} \left\{ \frac{bf(v)L\rho}{2\pi C_\rho C_A} \right\}^2. \quad (4)$$

The total stored energy in the material is

$$E_s = U_D + U_w. \quad (5)$$

It is assumed here that loop growth continues until a cellular dislocation microstructure forms, i.e.,

$$g(t) = C_A C_\rho \sqrt{\frac{\pi}{f(v)}} - d_l(t) \sqrt{\rho_d(t)} = 0, \quad (6)$$

where  $f(v) = \frac{1-v/2}{1-v}$ ,  $v$  is Poisson's ratio (0.31),  $C_A = 3$  for cubic cells,  $C_\rho$  is within a factor of 2 or so either way of unity, and  $d_l$  is assumed to equal to the cell size  $L$  at the point where the cellular dislocation network forms, i.e., when Eq. (6) is satisfied. The condition given by Eq. 6 is obtained by minimization of the total energy, i.e.,

$$\frac{d(U_w + U_D)}{dL} = 0. \quad (7)$$

Once Eq. 6 is satisfied, it is assumed that a stable cellular dislocation microstructure with a fixed cell size has been attained. In order to maintain the lowest energy configuration the continued pileup of dislocations on the cell walls will result in a decrease in cell size  $L$ .

### 3. Model for accumulation of forest dislocations and recrystallization

Two approaches were used to calculate immobile (forest) dislocation accumulation: the 1<sup>st</sup> based on a rate-theory model for loop interaction with forest dislocations located on cell walls (single-loop interaction model) and the 2<sup>nd</sup> model based on the interaction between two loops leading to the formation of immobile Lomer-Cottrell dislocations (two-loop interaction model). This latter model also considers the interaction of forest dislocations with mobile dislocations leading to their destruction.

The single-loop interaction rate-theory model [Rest, 1999] consists of a set of coupled differential equations for the time rate of change of the vacancy and interstitial concentrations, the interstitial loop diameter and density, the density of forest dislocations, the cavity radius and density, the average number of gas atoms in each cavity, and the concentration of gas atoms in solution in the fuel matrix.

Both approaches assume that the production of immobile dislocations cease at temperatures above that where dislocation annealing occurs.

Some examples of the kinetics of dislocation accumulation are shown in Fig.2 (two-loop interaction model) and 3 (single-loop interaction model).

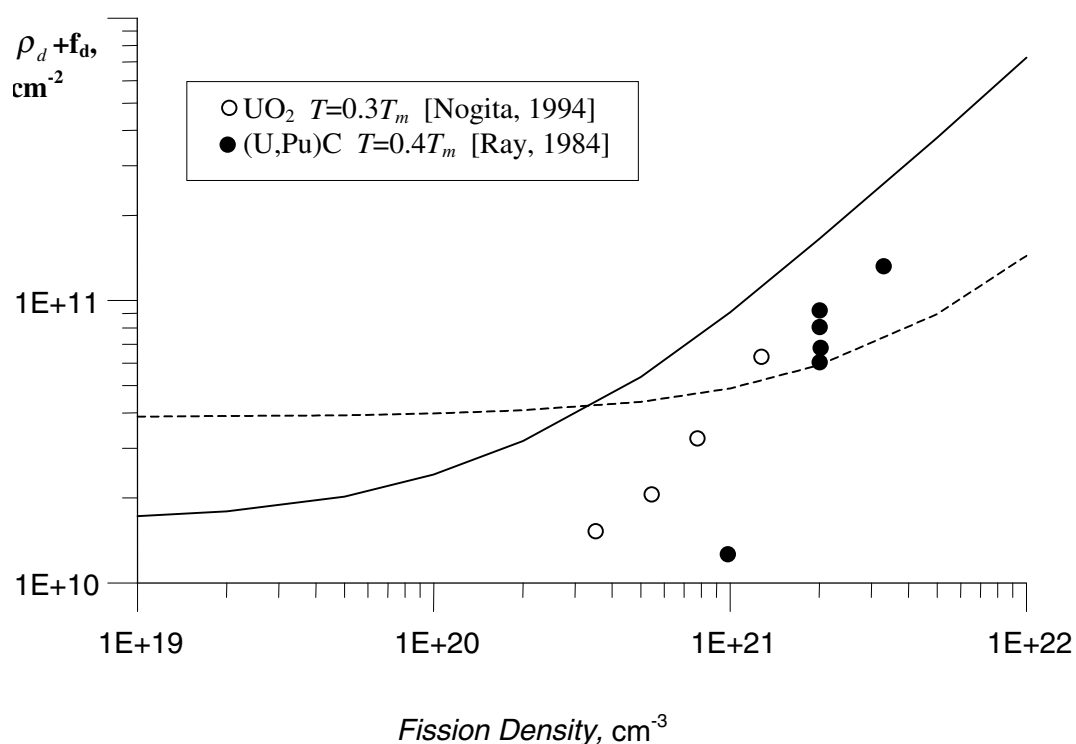


Fig.2. Calculated total dislocation density using the two-loop interaction model compared with data. The calculated data for  $\gamma$  uranium: continuous line - irradiation temperature of  $0.3T_m$ ,  $K=5.10^{-5}$  dpa/s; dotted line - irradiation temperature of  $0.4T_m$ ,  $K=5.10^{-4}$  dpa/s. The vacancy and interstitial migration energies used in the calculation are  $\epsilon_{vm} = 1.0$  eV and  $\epsilon_{im} = 0.15$  eV.

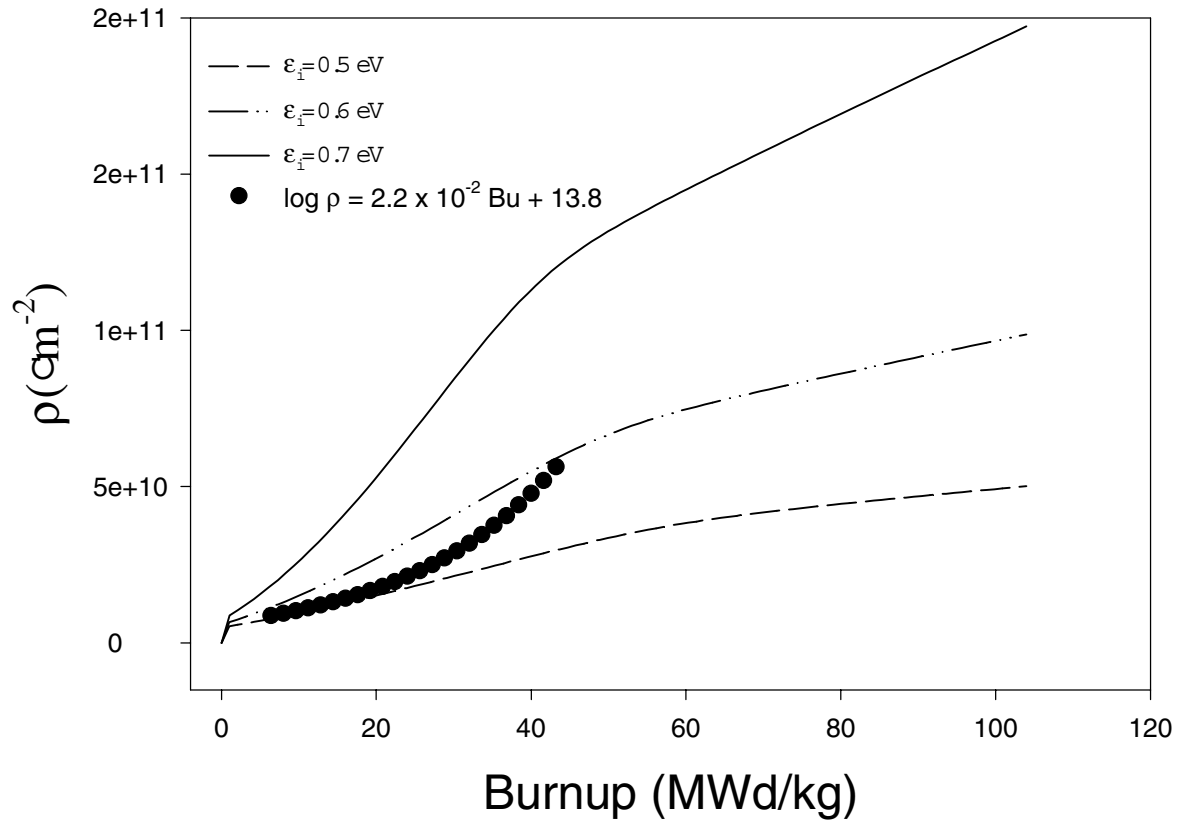


Fig. 2. Calculated total dislocation density  $\rho = \rho_d + f_d$  as a function of burnup using the single-loop interaction model. Also shown is fit (over the range of 6-44 MWd/kg) to measured dislocation density from Nogita, 1994.

The calculated dislocation density provided by both model approaches is in reasonable agreement with the data.

### Condition for recrystallization.

For a given value of the stored energy,  $E_s$ , nucleation of a new crystal of material results in a net change in free energy,  $\Delta G$ , given by

$$\Delta G = -E_s x^3 + 3\gamma x^2, \quad (8)$$

where  $\gamma$  is the surface energy density, and  $x(t)$  is the candidate grain diameter at time  $t$ . The first term on the right side of Eq. (8) is the decrease in free energy due to the creation of strain-free volume and the second term is the work required in order to create the grain boundary surface.  $\Delta G$  has an extremum (maximum) with respect to  $x$ , i.e.,

$$\frac{d\Delta G}{dx} = 0, \quad (9)$$

at a value of  $x$  given by  $x_{\max} = \frac{2\gamma}{E_s}$ , where the value of  $\Delta G$  at  $x_{\max}$  is  $\Delta G_{\max} = \frac{4\gamma^3}{E_s^2}$ . As  $E_s$  increases,  $x_{\max}$  and  $\Delta G_{\max}$  shift to smaller values. Subsequent to the formation of a cellular dislocation network, continued pileup of forest dislocations on the cell walls decreases the cell size according to Eq. (6) with the loop diameter,  $d_l$ , replaced by the cell size  $L$ . Recrystallization occurs when  $\Delta G_{\max}$  has achieved a minimum, i.e., when

$$x_{\max} = L, \quad (10)$$

i.e., the candidate grain size becomes the recrystallized grain size which is taken to be the cell size at that instant.

### **Mechanism of recrystallization.**

Using the classical energy approach to describe the formation of recrystallization nuclei, the critical radius  $R_c$  can be expressed as

$$R_c = \frac{3}{2} \cdot \frac{\gamma}{\Delta E}, \quad (11)$$

where  $\Delta E$  is the difference in energy between recrystallized material without dislocations, and pre-recrystallized material with a high dislocation density.

For edge dislocations with Burgers vector equal to  $a$ , the energy associated with the presence of dislocations can be derived from the classical approach of continuous matter as

$$\Delta E = \frac{G_s a^2}{4\pi(1-\nu)} \cdot \psi \quad (12)$$

where  $\psi = \rho_{dl} \ln \frac{\rho_{dl}^{-1/2}}{r_o}$ ,  $\rho_{dl}$  is the dislocation density on the cell border (approximately 10 times larger than the density referred to the entire volume of material), and  $r_o$  is the radius of a dislocation core (approximately equal to  $a$ ).

The final expression for the critical size of recrystallization nuclei for  $4\pi(1-\nu) \approx 10$ ,  $a \approx 3 \cdot 10^{-8}$  cm and  $\gamma / (G_s a) \approx 10^{-2}$  (the relation characteristic for metals) is [in cm]

$$R_c = 5 \cdot 10^6 / \psi . \quad (13)$$

Let us assume that a source of energy for “instant excitation” of a group of atoms for simultaneous reorganization into a nucleus is the energy transmitted by a fission fragment at the end its trajectory (thermal spike). The initiation of recrystallization is given by the condition  $\frac{4\pi}{3} R_c^3 < V_s$  where the volume of the thermal spike  $V_s \approx 10^{-17}$  cm<sup>3</sup>.

Figure 4 shows the calculated recrystallization dose as a function of temperature and damage rate made using the above stated conditions compared with data.

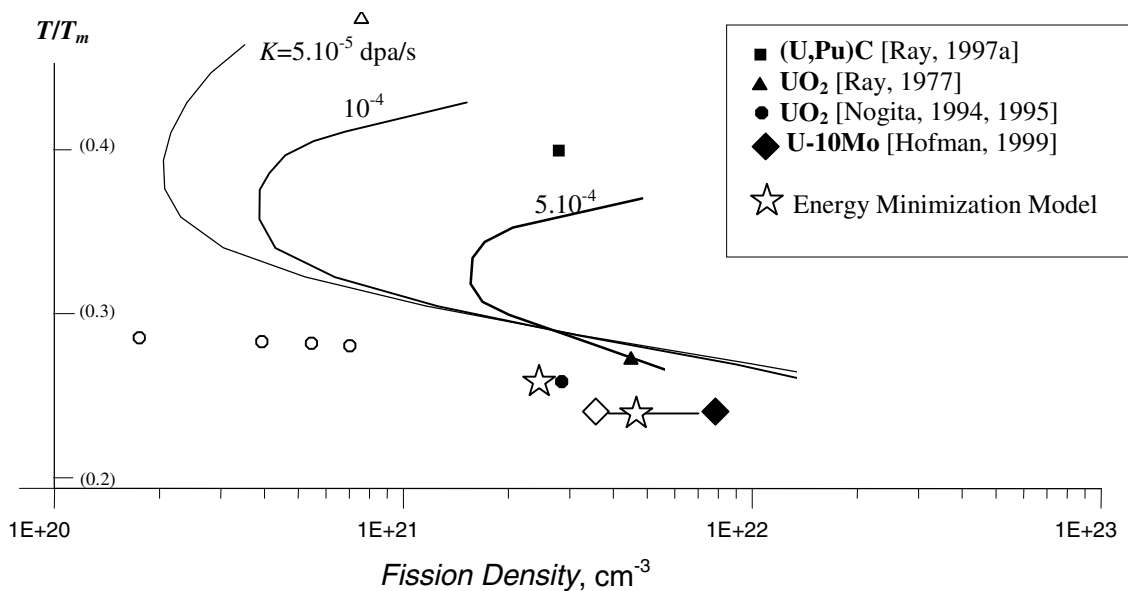


Fig.4. Calculated TTT-curves of irradiation induced recrystallization of uranium: recrystallization indicated by filled symbols, open symbols indicate absence of recrystallization. Also shown (star symbols) are the calculated recrystallization doses made using the energy-minimization model exemplified by Eqs. (6), (9), and (10).

The TTT-diagram (time-temperature-transformation) of recrystallization shown in Fig.4 is similar to phase transformation curves in alloys. The difference between the position of the nose of the calculated curves in Fig. 4 for different damage rates is associated with the number of available interstitials. The number of interstitials decreases with increasing damage rate due to interstitial loss mechanisms such as defect recombination.

Also shown in Fig. 4 are the calculated recrystallization doses for U-10Mo and UO<sub>2</sub> made using the energy-minimization model exemplified by Eqs. (6), (9), and (10). As shown in Fig. 4, the calculated doses are in reasonable agreement with the data.

Let us use classical nucleation and growth in order to calculate the number and size of recrystallized grains. On the cell walls, assumed to consist of one-tenth of the volume of the material, the production rate of recrystallized grains is given by

$$\frac{\partial N_R}{\partial t} = 0.1G \quad (14)$$

where  $G$  is the fission rate, and  $N_R$  is the density of recrystallization nuclei.

Let us define the growth rate of recrystallized grains,  $v_R$ , as

$$v_R = a v_v \exp(-1.0/kT)[1 - \exp(-\Delta E_a/kT)] \quad (15)$$

where  $\Delta E_a = \Delta E / N_a$  ( $N_a$  is the number of atoms in a unit of volume) is the difference in the energy of an atom between that in an ideal lattice, and that in a material deformed by dislocations. Taking into account the small value of  $\Delta E_a/kT$  and using a value for the frequency factor  $v_v = 10^{13} \text{ s}^{-1}$ ,

$$v_R = \frac{0.2}{kT} \exp(-1.0/kT) \psi \quad [\text{cm/s}] \quad (16)$$

Fig. 5 shows the calculated size of recrystallized grains using Eqs. (14) and (16) as a function of relative temperature compared with data. The calculation does not correspond to the trend of the data in that it predicts a much smaller recrystallized grain size than that observed at relative temperatures less than  $\approx 0.3$ .

Also shown in Fig. 5 are the calculated size of recrystallized grains made using the rate theory of dislocation formation and growth [Rest, 1999] coupled with the energy minimization approach exemplified by Eqs. (6), (9) and (10). The calculated quantities based on this approach are in good agreement with the measured quantities.

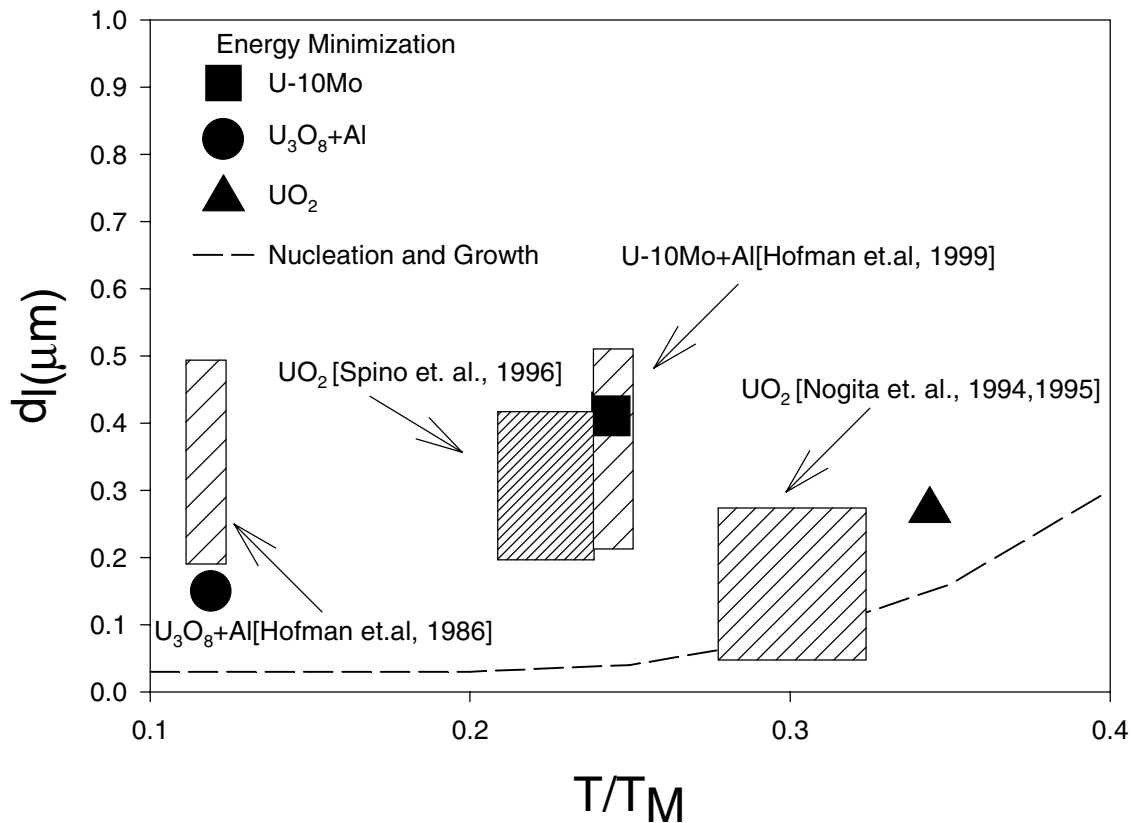


Fig. 5. Comparison of calculated diameter of recrystallized grains with data.

## Conclusions

The evolution of the dislocation structure and recrystallization have been identified as important aspects of the irradiated UMo alloy microstructure that can have a strong impact on fuel swelling. This paper presents several theoretical approaches for calculating the mobile and immobile dislocation density and subsequent recrystallization. The results of the analyses support a picture of recrystallization based on the accumulation of immobile (forest) dislocations on the walls of a cellular dislocation structure.

The results of the analyses do not support a classical nucleation and growth mechanism for irradiation-induced recrystallization phenomena. Instead, the formation of a cellular dislocation network relatively early in the irradiation followed by the buildup of immobile dislocations on the cell walls has been identified as the most likely mechanism. The buildup of immobile dislocations on the cell walls leads to an increase in the stored energy in the material. For high enough values of the stored energy, the system will have a thermodynamic preference to form new interfaces (boundaries) in order to reduce the strain energy within the bulk material.

In the absence of recrystallization, very high dislocation densities can lead to a vacancy supersaturation and bias-driven swelling. Bias-driven swelling, or void swelling, can lead to highly unstable fuel swelling. On the other hand, recrystallization, or grain-subdivision, results in the formation of a very ramified border structure that leads to the acceleration of point defect transport that is equivalent to an increase of irradiation temperature and may result in enhanced gas-bubble swelling. This type of swelling, however, is gas-driven and thus results in stable swelling behavior throughout the fuel operating temperature range (below the aluminum matrix melting temperature).

## REFERENCES

- Azam N., Le Naour L. and Delaplace J.** (1974) - J. Nucl. Mat., 49, p.197.
- Brown C. and Linecar G.** (1974) – “Dislocation Densities in ST and 20% Cold-Worked Type 316 Pin Cladding Irradiated to 30 dpa in PFR”. UKAEA TRG-Memo-6571.
- Buckley S.N.** (1966) – “Irradiation Growth in Uranium”. Report AERE-R 5262 (UK).
- Garner F.A., Wolfer W.G.** (1982), "A Model for the Evolution of Network Dislocation Density in Irradiated Metals", Effects of Irradiation on Materials: 11-th Conf. ASTM STP 782, p.1073.
- Garner F.A., Brager H.R., Gelles D.S., McCarthy J.M.** (1987) – J. Nucl. Mat., 148, p.294.
- Griffiths M.** (1988) – J. Nucl. Mat., 159, p.190.
- Hansen N. and Kuhlmann-Wilsdorf D.**, Mater. Sci. Eng., 81 (1986) 141.
- Hofman G. L., Copeland G. L., and Sanecke J. E.**, Nucl. Tech., 72 (3) (1986) 338.
- Hudson B., Westmacott K.H. and Makin M.J.** (1962) – Phil. Mag., 7, p.377.
- Hudson B.** (1964) – Phil. Mag., 10, p.949.
- Hudson B.** (1967) - J. Nucl. Mat., 22, p.121.
- Nogita K. and Une K.** (1994) – Nucl. Instr. and Meth. in Phys. Res. B 91 p.301.
- Nogita K. and Une K.** (1995) – J. Nucl. Mat., 226, p.302.
- Ray I.L. and Blank H.** (1984) – J. Nucl. Mat., 124, p.159.
- Ray I.L., Matzke H., Thiele H.A., Kinoshita M.** (1997) – J. Nucl. Mat., 245, p.115.
- Rest J and Hofman G.L.**, to be published in J. Nucl Mater (1999).
- Spino J., Vennix K., and Coquerelle M.**, J. Nucl. Mater. 231 (1996) 179.
- Agapova N.P., Ageev V.S., Antipina M.I. e.a.** (1982) – Questions of nuclear science and engineering. Series: Nuclear applied metallurgy, №4(15), p.19 (*in Russian*).
- Averin S.A., Shishov V.N., Antipina M.I. e.a.** (1999) – Questions of nuclear science and engineering. Series: Nuclear applied metallurgy, №1(56), p.21 (*in Russian*).